4-Methoxy-Substituted Poly(triphenylamine): A P-Type Polymer with Highly Photoluminescent and Reversible Oxidative Electrochromic Characteristics

GUEY-SHENG LIOU,[1] YI-LUNG YANG,[1] WEN-CHANG CHEN,[2] YUHLONG OLIVER SU[1]

[1]Department of Applied Chemistry, National Chi Nan University, 1 University Road, Nantou Hsien 54561, Taiwan, Republic of China

[2]Department of Chemical Engineering, National Taiwan University, Taipei, Taiwan 10617, Republic of China

Received 10 February 2007; accepted 7 March 2007
DOI: 10.1002/pola.22079
Published online in Wiley InterScience (www.interscience.wiley.com).

ABSTRACT: A 4-methoxy-substituted triphenylamine-containing homopolymer, poly [*N*,*N*-diphenyl-4-methoxyphenylamine-4′,4″-diyl] (**PMeOTPA**), with blue light (435 nm) fluorescence quantum efficiency up to 79% was easily prepared by oxidative coupling polymerization of *N*,*N*-diphenyl-4-methoxyphenylamine (**MeOTPA**) using $FeCl_3$ as an oxidant. Its reversible oxidation redox couple was at 0.41 V versus Fc/Fc^+ in acetonitrile solution. It exhibited good thermal stability with 10% weight-loss temperatures above 500 °C under a nitrogen atmosphere and relatively high softening temperature (154 °C). The simply designed homopolymer revealed moderate stability of electrochromic characteristics, changing color from original pale yellowish to red, and then to black. The **PMeOTPA** based field effect transistor also showed p-type characteristics with significant temperature dependence. The present study suggests that **PMeOTPA** is a multifunctional polymer for various optoelectronic device applications. © 2007 Wiley Periodicals, Inc. J Polym Sci Part A: Polym Chem 45: 3292–3302, 2007
Keywords: electrochemistry; fluorescence; functionalization of polymers; luminescence; polyamines

INTRODUCTION

Conjugated polymers have been extensively studied for their potential applications in electroluminescence displays,[1–3] photovoltaic devices,[4] and thin film transistors.[5] Arylamine-containing aromatics have attracted considerable interest as hole-transport materials in multilayer organic electroluminescence (EL) devices due to their relatively high mobilities and low ionization potentials.[6–10] The electroactive site of triphenylamine (TPA) is the nitrogen center, which is linked to three phenyl groups in a propeller-like geometry. The anodic oxidation pathway of TPA was well reported and the electrogenerated TPA cation radical dimerized to form tetraphenylbenzidine, which is more easily oxidized than the TPA molecule.[11] The electrochemical properties of TPA are affected when some of the hydrogen atoms are substituted with groups of different electronic strengths. In our previous studies, it was found that TPA revealed lower oxidation potential and the formed cation radical was stabilized when electro-donating groups (methyl, methoxy) were substituted at the *para*-phenyl position.[12–15] The feasibility of utilizing spin-coating and ink-jet printing processes for large-area EL devices and

Correspondence to: G.-S. Liou (E-mail: gsliou@ncnu.edu.tw) or Y. Oliver Su (E-mail: yosu@ncnu.edu.tw)

Journal of Polymer Science: Part A: Polymer Chemistry, Vol. 45, 3292–3302 (2007)

possibilities of various chemical modifications (to improve emission efficiencies and allow patterning) make polymeric materials containing triarylamine units very attractive.[16–24] To enhance the hole injection ability of polymeric emissive materials such as poly(1,4-phenylenevinylene)s (PPV) and polyfluorenes (PF), there have been several reports on PPV and PF derivatives involving hole-transporting units such as triarylamine or carbazole group in the emissive π-conjugated core/main chains[25–30] or grafting them as side chains in a polymer[31–33] or attaching them onto the polymer chain-ends or the outer surface of dendritic wedges.[34,35] However, the solubility of many highly conjugated polymers is low, particularly for blue-emitting species. These targeted blue-emitting polymers therefore often bear large alkyl, alkoxy, or aryloxy groups to improve solubility, thus lower their glass transition temperatures (T_gs) and thermal stability.

To obtain high T_g hole-transporting polymers, many investigators have prepared polymers containing TPA units in the main chain. Ogino and coworkers have successfully prepared TPA-containing polymers that had hole-transporting ability.[36,37] Murofushi and coworkers have also prepared a series of polytriphenylamines by carrying out Grignard reaction and then polymerizating the obtained Grignard reagent by using a nickel compound catalyst.[38–40] Kakimoto and coworkers reported that the charge injection and electroluminescent efficiency were improved remarkably by the incorporation of the hole-transporting polyimide containing a TPA moieties in the backbone.[41,42] Recently, we have reported the synthesis of soluble aromatic polyamides and polyimides bearing TPA units in the main chain.[43–48] Because of the incorporation of bulky, 3D TPA units along the polymer backbone, all the polymers were amorphous with good solubility in many aprotic solvents and exhibited excellent thin-film-forming capability. So far, polymeric triarylamines are prepared using copper-mediated Ullman reactions,[49] palladium[50–53] or nickel-catalyzed coupling reactions,[38–40,54–56] and nucleophilic substitution reactions.[57] However, these synthetic methods are not straightforward and require multiple steps to prepare the monomers. These findings prompted the development of another electrochemically stable hole-transporting polymer based on the oxidative coupling of TPA unit. We therefore design a novel *para*-methoxy substituted TPA-based conjugated homopolymer (**PMeOTPA**), which is a blue light (435 nm) emitter with fluorescence quantum efficiency up to 79%. The electrochemical, electrochromic, and photoluminescent properties of the polymer film prepared by casting solution onto an indium-tin oxide (ITO)-coated glass substrate are also investigated.

EXPERIMENTAL

Materials

Diphenylamine (ACROS), 4-iodoanisole (ALFA AESAR), copper powder (ACROS), potassium carbonate (SCHARLAU), triethyleneglycol dimethyl ether (TEGDME) (ALFA AESAR), iron (III) chloride (SHOWA), nitrobenzene (ACROS), *N*-methyl-2-pyrrolidinone (NMP) (TEDIA), *N,N*-dimethylacetamide (DMAc) (TEDIA), $CHCl_3$ (TEDIA), tetrahydrofuran (THF) (TEDIA), and hexamethyldisilazane (HMDS) (FLUKA) were used without further purification. Tetrabutylammonium perchlorate (TBAP) was obtained from ACROS and recrystallized twice from ethyl acetate and then dried *in vacuo* prior to use. All other reagents were used as received from commercial sources.

Preparation of (4-Methoxyphenyl)diphenylamine

A mixture of diphenylamine (4.23 g, 25 mmol), 4-iodoanisole (7.25 g, 31 mmol), copper powder (1.59 g, 25 mmol), potassium carbonate (6.91 g, 50 mmol), and triethyleneglycol dimethyl ether (TEGDME) (12.5 mL) was stirred under nitrogen atmosphere at 180 °C for 24 h. The reaction mixture was filtered and poured into ice water. The brown precipitate was collected by filtration, then recrystallized from methanol to give white crystalline (5.85 g, 85%); (mp = 108–110 °C; lit.[58] 104–105 °C by DSC at 10 °C/min). FTIR (KBr pellet, cm^{-1}): 1242, 1034 (aromatic —C—O—C— stretch). ^{1}H NMR (500 MHz, $CDCl_3$, δ, ppm): 3.85 (s, —OCH_3), 6.91 (d, 2H), 7.01 (t, 2H), 7.11 (d, 4H), 7.14 (d, 2H), 7.27 (t, 4H). ^{13}C NMR (125 MHz, $CDCl_3$, δ, ppm): 55.4, 114.7, 121.8, 122.8, 127.2, 129.0, 140.7, 148.1, 156.1. Anal. Calcd for $C_{19}H_{17}NO$ (275.34): C, 82.88%; H, 6.22%; N, 5.09%. Found: C, 82.90%; H, 6.22%; N, 5.02%.

Preparation of Poly[*N,N*-diphenyl-4-methoxyphenylamine-4′,4″-diyl]

In a 50-mL round-bottomed flask fitted with a three-way stopcock were placed **MeOTPA** (0.138 g,

0.5 mmol), $FeCl_3$ (0.203 g, 1.25 mmol), and nitrobenzene (1 mL) under nitrogen. The solution was stirred at room temperature for 24 h and poured into a mixture of methanol containing 10% hydrochloric acid. The precipitate was collected, washed with aqueous ammonium hydroxide, then dissolved in chloroform and filtered. The filtrate was poured into methanol to reprecipitate the polymer and dried *in vacuo* at 100 °C for 24 h (yield: 0.109 g, 80%). IR (KBr): 1240, 1034 (aromatic —C—O—C— stretch). ^{1}H NMR (500 MHz, DMSO-d_6, δ, ppm): 3.76 (s, —OCH_3), 6.95 (d, 2H), 6.97–7.01 (m, 6H), 7.06 (d, 4H), 7.09 (d, 2H), 7.27 (t, 4H), 7.51 (m, 4H). ^{13}C NMR (125 MHz, DMSO-d_6, δ, ppm): 55.1, 115.0, 115.1, 121.9, 122.1, 122.3, 122.5, 126.9, 127.4, 127.5, 129.3, 133.1, 139.6, 147.3, 156.1. Anal. Calcd for $(C_{19}H_{15}NO)_n$ (273.33): C, 83.49%; H, 5.53%; N, 5.12%. Found: C, 82.89%; H, 5.50%; N, 5.06%.

Preparation of Polymer Film

A solution of polymer was made by dissolving about 0.20 g of the **PMeOTPA** sample in 5 mL of DMAc. The homogeneous solution was poured into a 5-cm glass Petri dish, which was then placed in a 90 °C oven overnight to remove most of the solvent. The cast film was then released from the glass substrate and was further dried *in vacuo* at 170 °C for 8 h. The obtained film was about 30 μm in thickness and was used for solubility tests and thermal analyses.

Organic Field Effect Transistor Fabrication

The Organic thin film transistor was prepared from **PMeOTPA** with a bottom-contact configuration on the *p*-doped silicon wafers. A thermally grown 200 nm SiO_2 used as the gate dielectric with a capacitance of 17 nF/cm^2. The aluminum was used to create a common bottom-gate electrode. The source/drain regions were defined by a 10-nm thick chromium adhesion layer and a 100 nm thick gold contact electrode through a regular shadow mask, and the channel length (L) and width (W) were 25 and 1500 μm, respectively. Afterward, the substrate was modified with HMDS as silane coupling agents. The solution of **PMeOTPA** in DMAc was made with concentration of 0.5 wt %. Subsequently, this solution was filtered through 0.20-μm pore size polytetrafluoroethylene (PTFE) membrane syringe filters, spin-coated at a speed rate of 1000 rpm for 60 s onto the silanized SiO_2/Si substrate, and heated at 60 °C for 12 h in vacuum.

Measurements

Infrared spectra were recorded on a PerkinElmer RXI FT-IR spectrometer. Elemental analyses were run in an Elementar VarioEL-III. ^{1}H and ^{13}C NMR spectra were measured on a Bruker Avance 500 MHz FT-NMR system. Ultraviolet-visible (UV-vis) spectra of the polymer films were recorded on a Varian Cary 50 Probe spectrometer. Thermogravimetric analysis (TGA) was conducted with a PerkinElmer Pyris 1 TGA. Experiments were carried out on approximately 6–8 mg film samples heated in flowing nitrogen or air (flow rate = 20 cm^3/min) at a heating rate of 20 °C/min. Thermomechanical analysis (TMA) was conducted with a PerkinElmer TMA 7 instrument. The TMA experiments were conducted from 50 to 200 °C at a scanning rate of 10 °C/min with a penetration probe 1.0 mm in diameter under an applied constant load of 10 mN. Softening temperature (T_s) was taken as the onset temperatures of probe displacement on the TMA trace. Electrochemistry was performed with a CHI 611B electrochemical analyzer. Voltammograms are presented with the positive potential pointing to the right and with increasing anodic currents pointing upward. Cyclic voltammetry was conducted with the use of a three-electrode cell in which ITO (polymer films area about 0.7 cm × 0.5 cm) was used as a working electrode. A platinum wire was used as an auxiliary electrode. All cell potentials were taken with the use of a home-made Ag/AgCl, KCl (sat.) reference electrode. The spectroelectrochemical cell was composed of a 1-cm cuvette, ITO as a working electrode, a platinum wire as an auxiliary electrode, and a Ag/AgCl reference electrode. Absorption spectra were measured using an HP 8453 UV-visible spectrophotometer. Photoluminescence spectra were obtained from a Jasco FP-6300 spectrofluorometer. Output and transfer characteristics of the Organic Field Effect Transistor (OFET) devices were measured using Keithley 4200 semiconductor parametric analyzer. All the prepared procedures and electronic measurements are performed in ambient atmosphere.

RESULTS AND DISCUSSION

Synthesis and Characterization

A organosoluble aromatic polytriphenylamine, poly[*N*,*N*-diphenyl-4-methoxyphenylamine-4′,4″-diyl] (**PMeOTPA**), could be readily prepared by

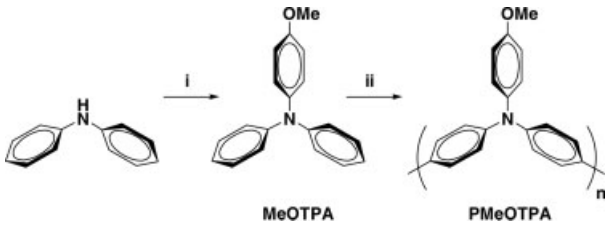

Scheme 1. Synthesis routes for **PMeOTPA**. *Reagents and conditions*: i, *p*-iodoanisole, Cu, K2CO3, TEGDME, 180 °C, 24 h; ii, $FeCl_3$, nitrobenzene, r.t., 24 h.

oxidative coupling polymerization of *N*,*N*-diphenyl-4-methoxyphenylamine (**MeOTPA**) using $FeCl_3$ as an oxidant.[59] The synthesis route and structure of **PMeOTPA** are shown in Scheme 1. The monomer compound (**MeOTPA**)[50] prepared by Ullmann coupling of diphenylamine with 4-iodoanisole is a violet light (371 nm) emitter with fluorescence quantum efficiency of 17%. The structures of monomer and polymer were confirmed by IR and NMR spectroscopy as shown in Figure 1, and the structural analysis of the **PMeOTPA** from NMR spectroscopy revealed exclusive 4′,4″-linkage between consecutive TPA repeat units on the polymer chains. The introduction of 4-methoxyphenyl group is expected to increase solubility of the TPA-containing polymer and also to enhance their electrochemical stability by substituent effect.[39–44] Thus, the resulting conjugated **PMeOTPA** showed good solubility in common organic solvents, such as chloroform and THF, and could be cast into a pale-yellowish free-standing film. The molecular weight of **PMeOTPA** was measured by gel permeation chromatography (GPC), using polystyrenes as standard and THF as eluent. The weight-average molecular weight (M_w) and polydispersity (PDI) were determined as 2000 and 2.06, respectively. **PMeOTPA** had useful levels of thermal stability, including 10% weight-loss temperatures beyond 500 °C and char yields at 800 °C in nitrogen higher than 68% associated with high softening temperature (154 °C) (Fig. 2). The high char yields of the polymers can be ascribed to their high aromatic content. Physical properties of the polymer were investigated with spectroscopic, thermal analysis, and electrochemical studies (Table 1).

Polymer Properties

Optical and Electrochemical Properties

The optical properties of **PMeOTPA** were investigated by UV–vis and fluorescence spectroscopy (Fig. 3). This polymer exhibited a maximum blue fluorescence at 435 nm in NMP solution with fluorescence quantum efficiency of 79%. The solid-state emission spectrum was similar to the

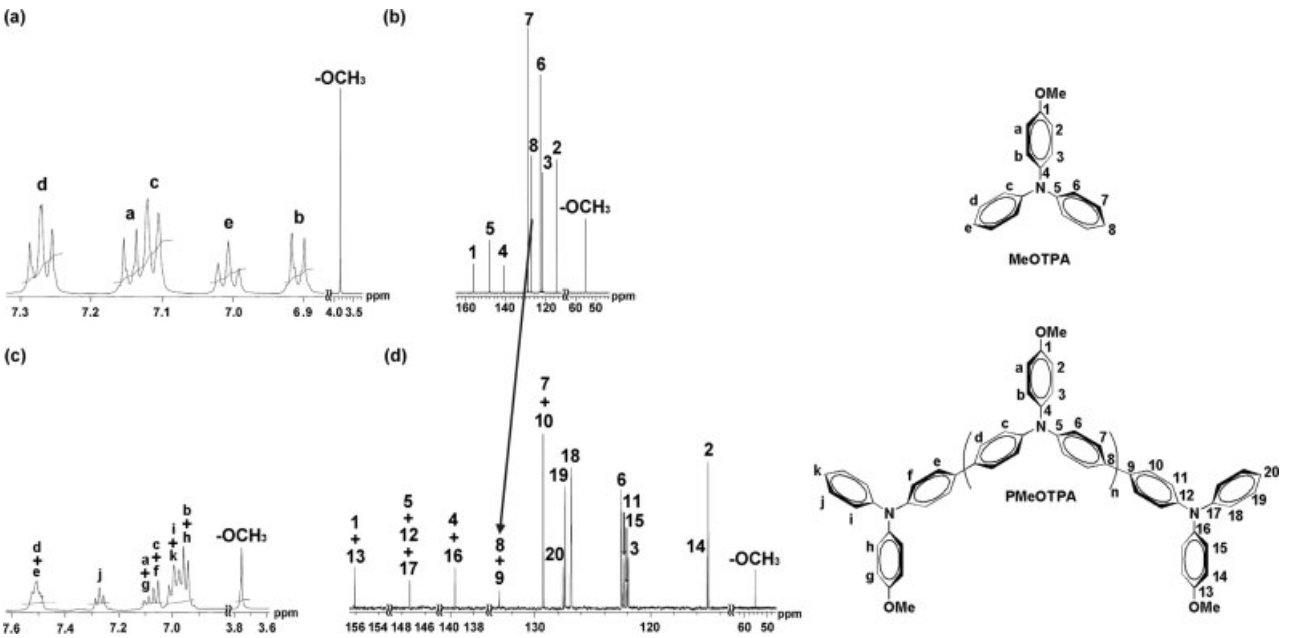

Figure 1. (a) ^1H NMR and (b) ^{13}C NMR spectra of MeOTPA in Chloroform-*d*; (c) ^1H NMR and (d) ^{13}C NMR spectra of PMeOTPA in DMSO-*d6*.

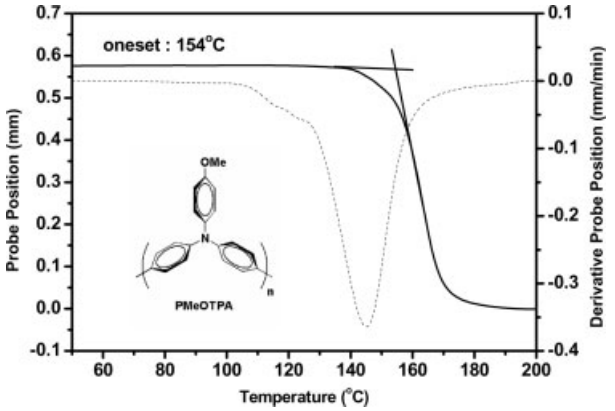

Figure 2. Typical TMA curve for PMeOTPA (heating rate = 10 °C /min; applied force = 10 mN).

recorded from the NMP solution. Although the solid-state of **PMeOTPA** was found to be slightly red shifted (11 nm) from the corresponding solution emission, the emission remained in the blue region. It can be attributed in part to the introduction of propeller-shaped TPA core in the repeat unit. The corresponding Highest Occupied Molecular Orbital (HOMO) and Lowest Unoccupied Molecular Orbital (LUMO) of **MeOTPA** optimized in the S_0 state could be predicted as shown in Figure 4. For the HOMO, π-conjugation of the orbital could be effectively extended to two phenyl groups. In contrast, the LUMO shows extension of π-conjugation over one of the phenyl groups, and the charge separation is localized only at the 4-methoxyphenyl and one of the phenyl groups. Accordingly, we illustrate the concept of π-conjugation in Figure 5. Optimized molecular geometry for **PMeOTPA** was obtained by minimizing energy via semiempirical Austin Model 1 (AM1) calculation in the gas state. AM1 is not only a semiempirical self-consistent field (SCF) method

Table 1. Physical Properties for **PMeOTPA**

Thermal Properties					
	T_d at 5% Weight Loss (°C)[b]		T_d at 10% Weight Loss (°C)[b]		Char Yield (wt %)[c]
T_s (°C)[a]	N_2	Air	N_2	Air	
154	460	455	500	500	68

Optical Properties						
NMP (1×10^{-5} M) Solution, r.t.			Film, r.t.			
λ_{abs} (nm)[d]	λ_{em} (nm)	Φ_F (%)[e]	λ_0 (nm)[f]	λ_{abs} (nm)	λ_{onset} (nm)	λ_{em} (nm)
(261), 291, 370[g]	435	78.7	430	371[g]	437	446

Electrochemical Properties					
Oxidation (V) (vs. Fc/Fc^+)			HOMO (eV)[i]	LUMO (eV)[j]	HOMO-LUMO Gap (eV)[k]
$E_{1/2}^{Ox,1h}$	$E_{1/2}^{Ox,2h}$	E_{onset}			
0.29 (0.44)[l]	0.45	0.13 (0.36)[l]	4.93	2.10	2.83

[a] Softening temperature measured by TMA with a constant applied load of 10 mN at a heating rate of 10 °C/min.
[b] Decomposition temperature, recorded via TGA at a heating rate of 20 °C/min and a gas-flow rate of 30 cm^3/min.
[c] Residual weight percentage at 800 °C in nitrogen.
[d] Value in parentheses is the highest absorption value of the UV–vis λ_{abs}.
[e] The value was measured by using 9,10-diphenylanthracene (dissolved in toluene with a concentration of 10^{-5} M, assuming fluorescence quantum efficiency of 0.90)[60] as a standard at 24–25 °C.
[f] The cutoff wavelengths (λ_0) from the transmission UV/Vis absorption spectra of polymer films 30 μm.
[g] Excitation wavelength for solution and/or film.
[h] The first and second half-wave potentials in CH_3CN containing 0.1 M TBAP.
[i] The HOMO energy level was calculated from cyclic voltammetry and was referenced to ferrocene (4.8 eV).
[j] LUMO = HOMO − gap.
[k] The data were calculated of thin film by the equation: gap = $1240/\lambda_{onset}$.
[l] 10^{-3} M MeOTPA in CH_3CN containing 0.1 M TBAP.

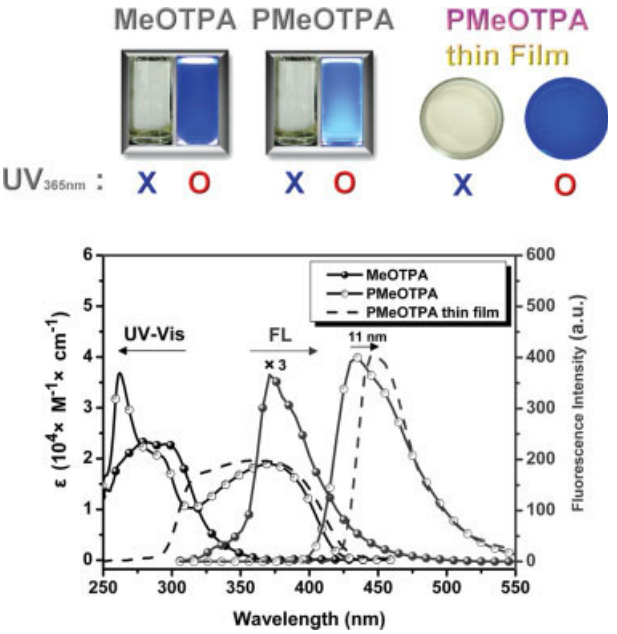

Figure 3. Molar absorptivity (left) and fluorescence intensity (right) of MeOTPA (●), PMeOTPA (○) in NMP solution (ca. 1×10^{-5} M), and PMeOTPA thin film (dashed line). a.u., arbitrary units. [Color figure can be viewed in the online issue, which is available at www.interscience.wiley.com.]

for chemical calculations but also an improvement of the modified neglect of differential diatomic overlap (MNDO) method. Together with Parameterized Model number 3 (PM3), AM1 is generally the most accurate semiempirical method and useful for molecules containing elements from long Rows 1 and 2 of the periodic table. The molecular model was implemented in the Hyperchem molecular graphics package.[62] Since each of TPA group in **PMeOTPA** is twisted from another TPA segment at 37.8 °, it could be suggested that the twisted structure between

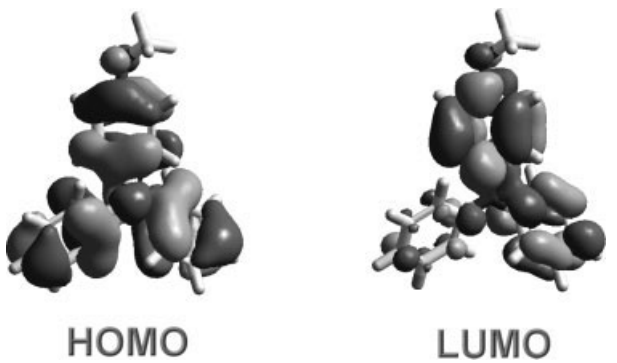

Figure 4. HOMO and LUMO of MeOTPA as indicated. The geometries were optimized at the Austin Model 1 (AM1)[61] semiempirical method.

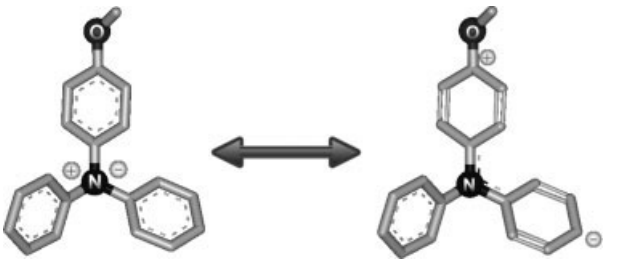

Figure 5. Electronic resonance structures of MeOTPA in the $^1(\pi,\pi^*)$ state.

repeat segments in **PMeOTPA** could not efficiently limit delocalization of electronic charges. Therefore, the delocalized electron coupling can interpret intervalence charge-transfer (IV-CT) absorption spectra within two electoractive nitrogen redox centers between the repeat TPA units of **PMeOTPA**, and show two different oxidation potentials from cyclic voltammetric scanning (Fig. 7).[63] Although only a single conformation is observed for the optimized molecular geometry of **PMeOTPA**, it is possible that the relaxation of packing constraints in solution might allow other conformations to be present. Therefore, a molecular mechanic study was undertaken to determine

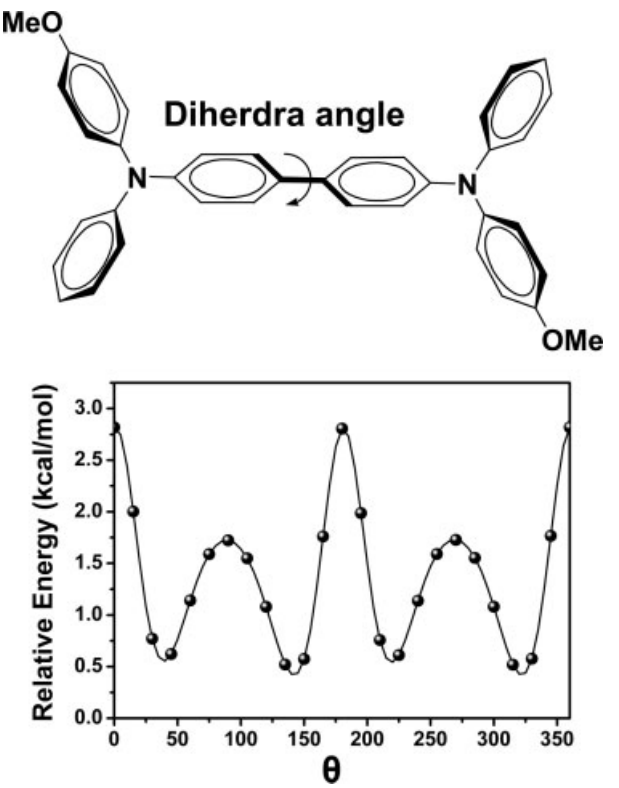

Figure 6. Potential energy of PMeTPA as a function of the dihedral angle θ.

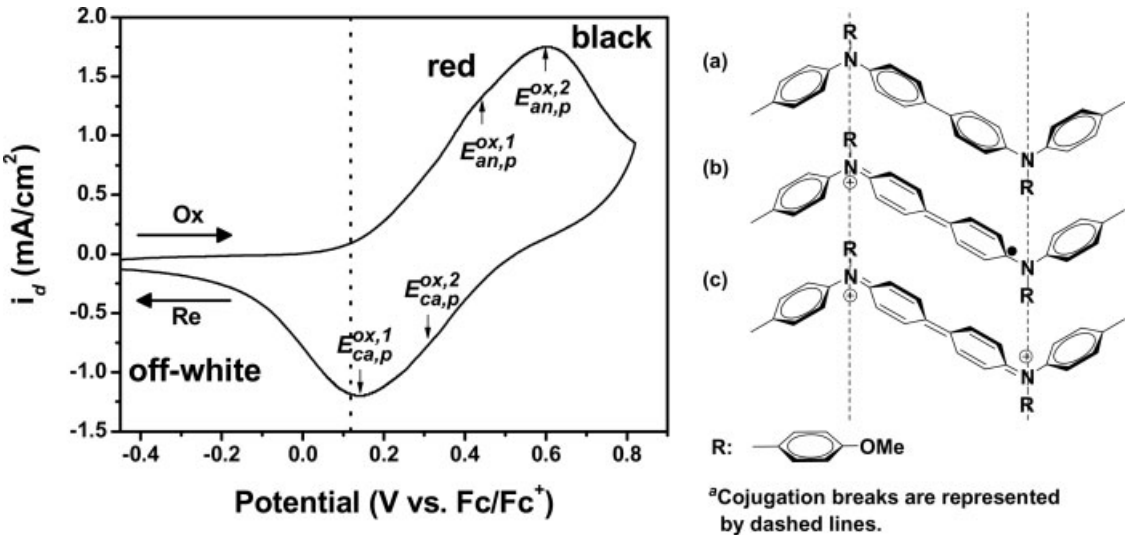

Figure 7. Cyclic voltammogram of PMeOTPA. Working electrode: PMeOTPA film coated on indium-tin oxide (ITO) glass plate (square, ca. 0.70 cm^2) in CH_3CN containing 0.1 M TBAP; counter electrode: platinum wire; reference electrode: Ag/AgCl. Scan rate: 0.1 V/s at room temperature. The arrows indicate the film color change during scan. E_{onset} value is indicated by a dotted line. A segment of PMeOTPA (a) neutral state, (b) radical cation state, and (c) dication state.

the potential energy (in kcal/mol) of the molecule as a function of the dihedral angle θ, and the results are plotted in Figure 6.

Electrochromic Characteristics

Electrochromic materials exhibit different colors depending upon the oxidation state. The applications for electrochromic conjugated polymers are quite diverse due to several favorable properties of these materials. Since the various oxidation states of conjugated polymers are quite stable and long-lasting. In addition, conjugated polymeric electrochromics usually show fast switching, allowing for rapid color changes from the materials upon appropriate applying potentials.[64–67] **PMeOTPA** is electrochemically stable and the anodic oxidation pathway was also postulated in Figure 7. The highest occupied molecular orbital (HOMO) and lowest unoccupied molecular orbital (LUMO) energy levels of the polymer can be determined from the oxida-

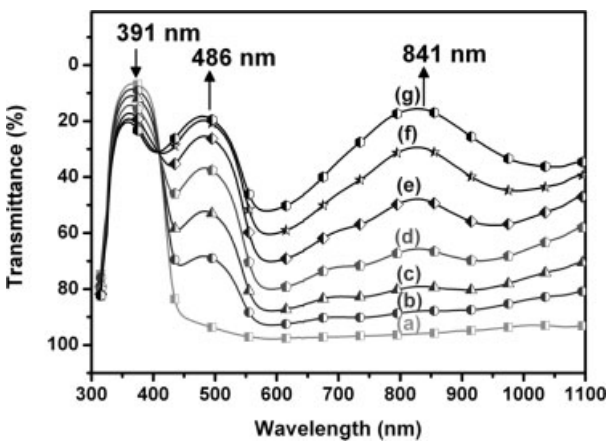

Figure 8. Electrochromic behavior of PMeOTPA thin film (in CH_3CN with 0.1 M TBAP as the supporting electrolyte) at (a) −0.48, (b) 0.19, (c) 0.30, (d) 0.41, (e) 0.52, (f) 0.63, and (g) 0.79 (V vs. Fc/Fc$^+$).

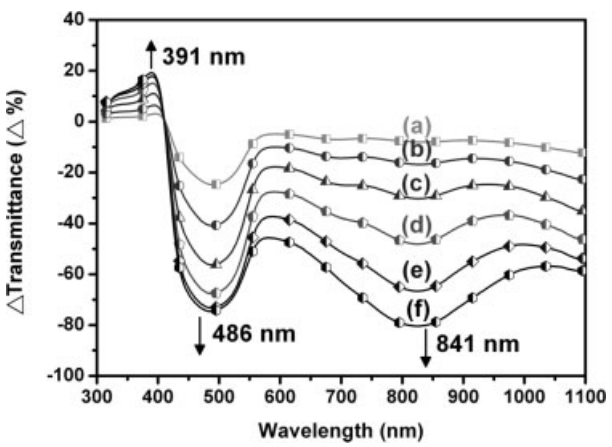

Figure 9. Electrochromic behavior of PMeOTPA thin film (in CH_3CN with 0.1 M TBAP as the supporting electrolyte) at (a) 0.19 (b) 0.30 (c) 0.41 (d) 0.52 (e) 0.63, and (f) 0.79 (V vs. Fc/Fc$^+$).

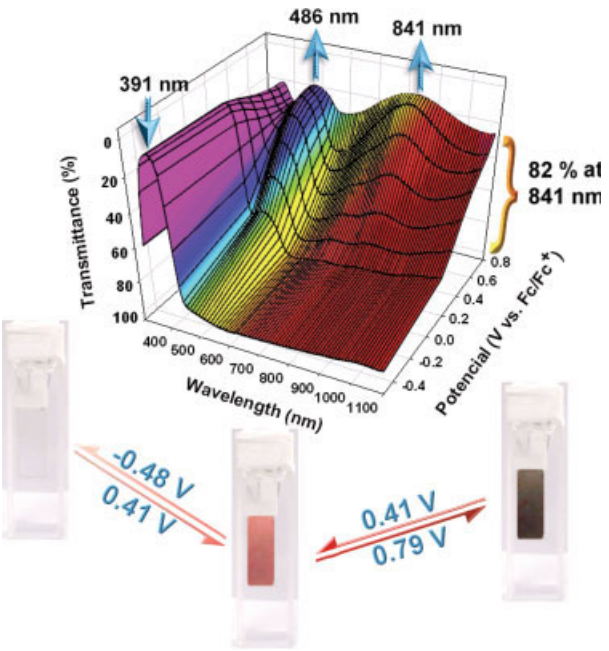

Figure 10. (a) Electorchromic behavior of PMeOTPA thin film (in CH_3CN with 0.1 M TBAP as the supporting electrolyte from −0.48 to 0.79 (V vs. Fc/Fc^+).

tion onset potentials of cyclic voltammetry and the onset absorption wavelength.

Spectroelectrochemical analysis of the **PMeOTPA** film was carried out on an ITO-coated glass substrate, and it showed multicolor electrochromic behavior when the applied potential was adjusted. The color of the polymer was changed from neutral pale-yellowish to red, and then to black. The typical spectroelectrochemical spectra of **PMeOTPA** at various applied potentials are depicted in Figures 8 and 9. When the applied potentials was increased positively from −0.48 to 0.79 (V vs. Fc/Fc^+), the characteristic absorbance at 391 nm decreased gradually while two new bands grew up at 486 and 841 nm due to the electron oxidation. The new spectrum was assigned as that of the stable cationic radical **PMeOTPA**$^{+\cdot}$, and the film color changed from pale yellow to black. Furthermore, the transmittance modulation at 841 nm gave the largest value, ca. 82% as shown in Figure 10. The coloration efficiency at 841 nm is as high as ca. 257 cm^2/C with high optical density change (ΔOD) up to 0.66, determined from the *in situ* experiments.[68]

The stability and response time upon electrochromic switching of the polymer film between its neutral and oxidized forms was monitored (Fig. 11). The switching time was defined as the time that required for reach 90% of the full change in

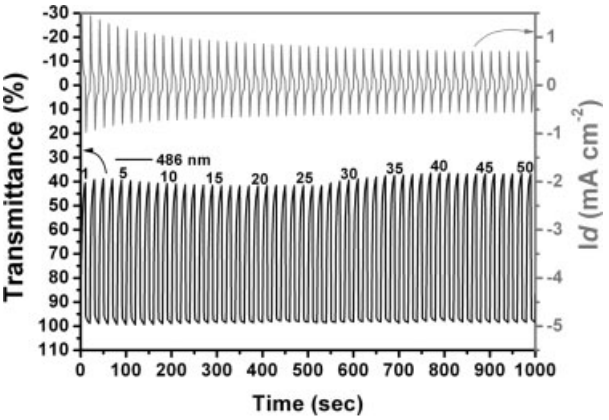

Figure 11. Potential step absorptometry and current consumption of PMeOTPA by applying potential steps −0.48 to 0.41 (V vs. Fc/Fc^+) with coloration efficiency (CE = 250 cm^2/C), (coated area: 0.70 cm^2)) and cycle time 20 s.

absorbance after switching potential. **PMeOTPA** would require 5.05 s at 0.41 V vs. Fc/Fc^+ for switching transmittance at 486 nm and 0.81 s for bleaching. After over continuous 50 cyclic switches between −0.48 and 0.41 V, the polymer

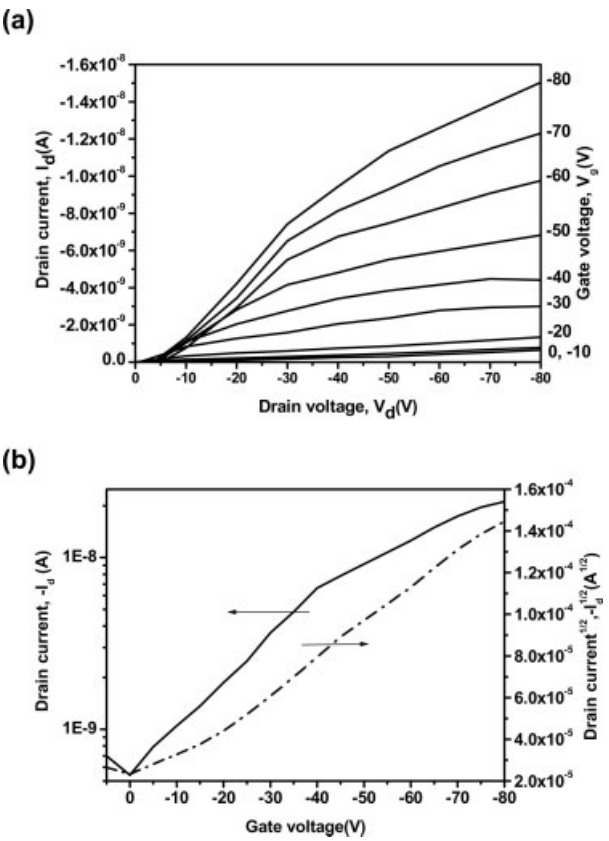

Figure 12. The (a) output and (b) transfer characteristics of a PMeOTPA OTFT before annealed.

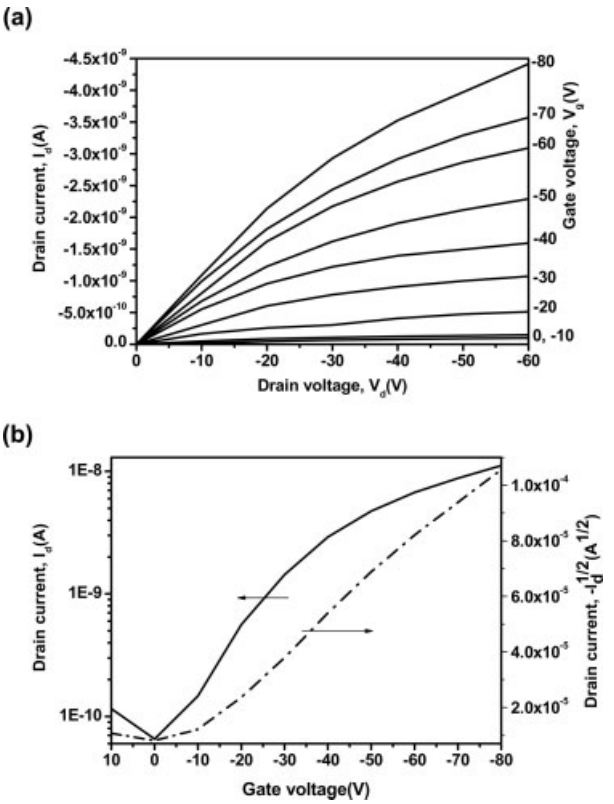

Figure 13. The (a) output and (b) transfer characteristics of a PMeOTPA OTFT annealed at 160 °C for 30 min.

films still exhibited moderate stability of electrochromic characteristics.

Organic Field Effect Transistor Characteristics

Figures 12 and 13 show the field effect transistor characteristics of the **PMeOTPA**. The I-V curve shows that the **PMeOTPA** based thin-film transistor has the p-type characteristics with the accumulation operation. In the saturation region ($V_d > V_g - V_t$), the drain current I_d can be described by the following equation:[69]

$$I_d = \left(\frac{WC_o\mu_h}{2L}\right)(V_g - V_t)^2 \qquad (1)$$

where μ_h is the hole mobility in the saturation region, C_o is the capacitance per unit area of the gate dielectric layer (SiO_2, 200 nm, $C_o = 17$ nF cm^{-2}), W is the channel width, L is the channel length, and V_t is the threshold voltage ($V_t = 5$ V). The field-effect mobility of the saturation region was calculated from the transfer characteristics of the **PMeOTPA** FET. A saturation hole mobility of 5.8×10^{-6} cm^2 V^{-1} s^{-1} with an on/off ratio of 50 was observed in the FET with the HMDS treatment. A similar device annealed at 160 °C for 30 min gave a hole mobility of 3.7×10^{-6} cm^2 V^{-1} s^{-1} and an on/off ratio of 170. The decrease of the hole mobility and increase of an on/off ratio indicate that the morphology of the **PMeOTPA**/HMDS interface in these FET is very sensitive to the annealing temperature, which is similar to our previous report on the poly(thiophene-2,5-diyl-alter-(2,3-diheptylquinoxaline-5,8,-diyl).[70] The softening temperature of the **PMeOTPA** is around 154 °C and thus the interface structure might be modified for the high annealing temperature.

CONCLUSIONS

These results presented herein also demonstrated that incorporating *para*-methoxy group into polymer backbone not only enhanced the processability of the triphenylamine polymer while maintaining good thermal stability, but also revealed higher HOMO energy level, excellent electrochemical stability, and highly electrochromic contrast characteristics. Thus, our novel main-chain triphenylamine-containing polymer can be employed as potential candidates in the development of dynamic electrochromic and EL devices due to their proper HOMO value, excellent thermal stability, and reversible electrochemical behavior.

The authors are grateful to the National Science Council of the Republic of China for financial support of this work.

REFERENCES AND NOTES

1. Akcelrud, L. Prog Polym Sci 2003, 28, 875.
2. Kim, D. Y.; Cho, H. N.; Kim, C. Y. Prog Polym Sci 2000, 25, 1089.
3. Tao, X.-T.; Zhang, Y.-D.; Wada, T.; Sasabe, H.; Suzuki, H.; Watanabe, T.; Miyata, S. Adv Mater 1998, 10, 226.
4. Hou, J.; Yang, C.; Heab, C.; Li, Y. Chem Commun 2006, 871.
5. Muccini, M. Nat Mater 2006, 5, 605.
6. Tang, C.-W.; VanSlyke, S.-A. Appl Phys Lett 1987, 51, 913.
7. Tang, C.-W.; VanSlyke, S.-A.; Chen, C.-H. J Appl Phys 1989, 85, 3610.

8. Adachi, C.; Nagai, K.; Tamoto, N. Appl Phys Lett 1995, 66, 2679.
9. Shirota, Y. J Mater Chem 2000, 10, 1.
10. Shirota, Y. J Mater Chem 2005, 15, 75.
11. Seo, E. T.; Nelson, R. F.; Fritsch, J. M.; Marcoux, L. S.; Leedy, D. W.; Adams, R. N. J Am Chem Soc 1966, 88, 3498.
12. Yeh, S.-J.; Tsai, C.-Y.; Huang, C.-Y.; Liou, G.-S.; Cheng, S.-H. Electrochem Commun 2003, 5, 373.
13. Chiu, K.-Y.; Su, T.-H.; Li, J.-H.; Lin, T.-H.; Liou, G.-S.; Cheng, S.-H. J Electroanal Chem 2005, 575, 95.
14. Chiu, K.-Y.; Su, T.-H.; Liou, G.-S.; Cheng, S.-H. J Electroanal Chem 2005, 575, 283.
15. Hawker, C. J.; Wooley, K. L. Science 2005, 309, 1200.
16. Bellmann, E.; Shaheen, S.-E.; Thayumannvan, S.; Barlow, S.; Grubbs, R. H.; Marder, S. R.; Kippelen, B.; Peyghambarian, N. Chem Mater 1998, 10, 1668.
17. Bellmann, E.; Shaheen, S.-E.; Grubbs, R. H.; Marder, S.-R.; Kippelen, B.; Peyghambarian, N. Chem Mater 1999, 11, 399.
18. Lu, J.-P.; Hlil, A.-R.; Sun, Y.; Hay, A.-S.; Maindron, T.; Dodelet, J.-P.; D'Iorio, M. Chem Mater 1999, 11, 2501.
19. Wang, X.-Q.; Nakao, M.; Ogino, K.; Sato, H.; Tan, H. M. Macromol Chem Phys 2001, 202, 117.
20. Wang, X.-Q.; Chen, Z. J.; Ogino, K.; Sato, H.; Strzelec, K.; Miyata, S.; Luo, Y. J.; Tan, H. M. Macromol Chem Phys 2002, 203, 739.
21. Fang, Q.; Yamamoto, T. Macromolecules 2004, 37, 5894.
22. Xiao, H.-B.; Leng, B.; Tian, H. Polymer 2005, 46, 5705.
23. Cho, J.-S.; Kimoto, A.; Higuchi, M.; Yamamoto, K. Macromol Chem Phys 2005, 206, 635.
24. Sun, M.-H.; Li, J.; Li, B.-S.; Fu, Y.-Q.; Bo, Z.-S. Macromolecules 2005, 38, 2651.
25. Liu, Y.-Q.; Liu, M.-S.; Li, X.-C.; Jen, A. K.-Y. Chem Mater 1998, 10, 3301.
26. Li, X.-C.; Liu, Y.-Q.; Liu, M.-S.; Jen, A. K.-Y. Chem Mater 1999, 11, 1568.
27. Redecker, M.; Bradley, D.-D.-C.; Inbasekaran, M.; Wu, W.-W.; Woo, E.-P. Adv Mater 1999, 11, 241.
28. Ego, C.; Grimsdale, A.-C.; Uckert, F.; Yu, G.; Srdanov, G.; Mullen, K. Adv Mater 2002, 14, 809.
29. Shu, C.-F.; Dodda, R.; Wu, F.-I.; Liu, M. S.; Jen, A. K.-Y. Macromolecules 2003, 36, 6698.
30. Wu, F.-I.; Shih, P.-I.; Shu, C.-F.; Tung, Y.-L.; Chi, Y. Macromolecules 2005, 38, 9028.
31. Pu, Y.-J.; Soma, M.; Kido, J.; Nishide, H. Chem Mater 2001, 13, 3817.
32. Liang, F.-S.; Pu, Y.-J.; Kurata, T.; Kido, J.; Nishide, H. Polymer 2005, 46, 3767.
33. Liang, F.-S.; Kurata, T.; Nishide, H.; Kido, J. J Polym Sci Part A: Polym Chem 2005, 43, 5765.
34. Miteva, T.; Meisel, A.; Knoll, W.; Nothofer, H.-G.; Scherf, U.; Muller, D.-C.; Meerholz, K.; Yasuda, A.; Neher, D. Adv Mater 2001, 13, 565.
35. Fu, Y.-Q.; Li, Y.; Li, J.; Yan, S.-K.; Bo, Z.-S. Macromolecules 2004, 37, 6395.
36. Son, J. M.; Mori, T.; Ogino, K.; Sato, H.; Ito, Y. Macromolecules 1999, 32, 4849.
37. Ogino, K.; Kanegae, A.; Yamaguchi, R.; Sato, H.; Kurjata, J. Macromol Rapid Commun 1999, 20, 103.
38. Murofushi, Y.; Ishikawa; M.; Kawai, M. U.S. Patent 4,565,860, 2001.
39. Ohsawa, Y.; Ishikawa, M.; Miyamoto, T.; Murofushi, Y.; Kawai, M. Synth Met 1987, 18, 371.
40. Ishikawa, M.; Kawai, M.; Ohsawa, Y. Synth Met 1991, 40, 231.
41. Nishikata, Y.; Fukui, S.; Kakimoto, M.; Imai, Y.; Nishiyama, K.; Fujihira, M. Thin Solid Films 1992, 210/211, 296.
42. Wu, A.; Jikei, M.; Kakimoto, M.; Imai, Y.; Ukishima, Y. S.; Takahashi, Y. Chem Lett 1994, 2319.
43. Liou, G.-S.; Hsiao, S.-H.; Huang, N.-K.; Yang, Y.-L. Macromolecules 2006, 39, 5337.
44. Cheng, S.-H.; Hsiao, S.-H.; Su, T.-H.; Liou, G.-S. Macromolecules 2005, 38, 307.
45. Liou, G.-S.; Yang, Y.-L.; Su, Y. O. J Polym Sci Part A: Polym Chem 2006, 44, 2587.
46. Liou, G.-S.; Huang, N.-K.; Yang, Y.-L. J Polym Sci Part A: Polym Chem 2006, 44, 4095.
47. Liou, G.-S.; Huang, N.-K.; Yang, Y.-L. Polymer 2006, 47, 7013.
48. Liou, G.-S.; Hsiao, S.-H.; Chen, H.-W.; Yen, H.-J. J Polym Sci Part A: Polym Chem 2006, 44, 4108.
49. Schmitz, C.; Thelakkat, M.; Schmidt, H.-W. Adv Mater 1999, 11, 821.
50. Goodson, F. E.; Hauck, S. I.; Hartwig, J. F. J Am Chem Soc 1999, 121, 7527.
51. Yu, W. L.; Pei, J.; Huang, W.; Heeger, A. J. Chem Commun 2000, 681.
52. Lim, E.; Kim, Y. M.; Lee, J.-I.; Jung, B.-J.; Cho, N. S.; Lee, J.; Do, L.-M.; Shim H.-K. J Polym Sci Part A: Polym Chem 2006, 44, 4709.
53. Lim, E.; Jung, B.-J.; Shim, H.-K. J Polym Sci Part A: Polym Chem 2006, 44, 243.
54. Tanaka, S.; Iso, T.; Doke, Y. Chem Commun 1997, 2063.
55. Lee, S. K.; Ahn, T.; Cho, N. S.; Lee, J.-I.; Jung, Y. K.; Lee, J.; Shim, H. K. J Polym Sci Part A: Polym Chem 2007, 45, 1199.
56. Kim, Y.-H.; Zhao, Q.; Kwon, S.-K. J Polym Sci Part A: Polym Chem 2006, 44, 172.
57. Kido, J.; Hamada, G.; Nagai, K. Polym Adv Technol 1996, 7, 31.
58. Paine, A. J. J Am Chem Soc 1987, 109, 1496.
59. Nomura, M.; Shibasaki, Y.; Ueda, M. Macromolecules 2004, 37, 1204.
60. Hamai, S.; Hirayama, F. J Phys Chem 1983, 87, 83.
61. Dewar, M. J. S., Zoebisch, E. G.; Healy, E. F.; Stewart, J. J. P. J Am Chem Soc 1985, 107, 3902.

62. Hypercube. Hyperchem Version 7.5; Hypercube: Gainesville, FL, 2003.
63. Lambert, C.; Nöll, G. J Am Chem Soc 2005, 121, 8434.
64. Sonmez, G. Chem Commun 2005, 5251.
65. Sonmez, G.; Shen, C. K. F.; Rubin, Y.; Wudl, F. Angew Chem Int Ed 2004, 43, 1498.
66. Sonmez, G.; Sonmez, H. B.; Shen, C. K. F.; Wudl, F. Adv Mater 2004, 16, 1905.
67. Sonmez, G.; Wudl, F. J Mater Chem 2005, 15, 20.
68. Argun, A. A.; Aubert, P.-H.; Thompson, B. C.; Schwendeman, I.; Gaupp, C. L.; Hwang, J.; Pinto, N. J.; Tanner, D. B.; MacDiarmid, A. G.; Reynolds, J. R. Chem Mater 2004, 16, 4401.
69. Babel, A.; Jenekhe, S. A. J Phys Chem B 2003, 107, 1749.
70. Champion, R. D.; Cheng, K. F.; Pai, C. L.; Chen, W. C.; Jenekhe, S. A. Macromol Rapid Commun 2005, 26, 1835.